Developments in the Built Environment 16 (2023) 100185

Contents lists available at ScienceDirect

Developments in the Built Environment

journal homepage: www.sciencedirect.com/journal/developments-in-the-built-environment

Thermal improvements of box-window using shading attachments. Hot-box measurements

Cezary Misiopecki [a,*], Steinar Grynning [b], Arild Gustavsen [a]

[a] Department of Architectural Design, History and Technology, Norwegian University of Science and Technology (NTNU), NO-7491, Trondheim, Norway
[b] Department of Materials and Structures, SINTEF Building and Infrastructure, NO-7465, Trondheim, Norway

ARTICLE INFO

Keywords:
Window
Window attachments
Shading
Cellular shade
Roller-shades
Box-window
Hot-box
Laboratory
Heritage
Energy retrofit

ABSTRACT

This research explores shading potential for improving the thermal properties of a box-window. Two different types of shades along with three placements were considered. Ten configurations were tested in a hot-box apparatus and compared to base window performance. Condensation issues that may arise after shading installation were also studied.

Measurements showed that shading installed along with the original box-window has a positive impact on the window thermal performance. The highest U-value reduction by 35% (from 1.9 to 1.0 W/m^{2}K) was achieved by a roller-shade with low-emissivity layer and constrained airflow on shade perimeter, installed inside the window recess. Temperature analysis showed a higher risk of condensation on the indoor window surface due to shade introduction on the indoor side of the window.

Shading placement within the box-window gave improvements of 34% (reduced U-value from 2.0 to 1.3 W/m^{2}K) for reflective roller-shades placed between the window frames. Shades in this position do not increase the risk of condensation on the indoor surface of the window. The probability of condensation inside the box-window may be lowered by draught-proofing indoor frames and maintaining ventilation through the outdoor frame.

Shades proved to be effective at improving the thermal properties of box-windows.

1. Introduction

1.1. General

If global development and associated use of fossil fuels continues at the current pace, it may lead to serious consequences for the climate. Energy use in buildings is important since it is responsible for 35% of the final energy consumption and 33% of global CO_2 emissions (International Energy Agency, 2013) (Gray, 2007). The International Energy Agency forecasts that existing buildings will use most of the energy consumed by all buildings in the future. Predictions show that new building constructions will only contribute to an additional 10%–20% of the total sector's energy consumption by 2050 in most of the industrialized countries (Schwehr et al., 2011). Existing buildings may still be functional, occupied and in prime locations. Many of them have heritage value and should be preserved. All these reasons make existing buildings difficult to replace. In the European Union, around 23% of the current building stock was built before 1945 and many of these buildings have a heritage significance; thus, there should be a strong focus on retrofitting strategies that provide energy savings for existing buildings (Dol and Haffner, 2010) (Mazzarella, 2015) (Oliveira et al., 2017) (Bertone et al., 2016).

Windows have a crucial role in defining the style and character of an individual building. Their materials and technical solutions represent the historic style of a building. Based on fenestration features, i.e. size, articulation, subdivision and formal variations, building age can be determined with an accuracy of 10–20 years. Thus, historic windows should be respected as an integral part of the architectural heritage of a building (Lorinczi, 2005) (Sedovic and Gotthelf, 2005). Fenestration causes relatively high heat losses through the building envelope since their thermal transmittance remains significantly higher than for walls (Gustavsen et al., 2008). This all motivates further research into new solutions and retrofitting strategies with minimal impact on the appearance of windows in heritage buildings.

A box-type double sash window is a common window construction that can be found in existing buildings throughout Northern Europe. In the nineteenth century, it became common to fit single-pane windows with a secondary frame, which was added during the winter period to

* Corresponding author. Department of Architectural Design, History and Technology, NTNU, Alfred Getz vei 3, 7491, Trondheim, Norway.
E-mail address: cezary.misiopecki@ntnu.no (C. Misiopecki).

https://doi.org/10.1016/j.dibe.2023.100185
Received 1 March 2023; Received in revised form 1 June 2023; Accepted 9 June 2023
Available online 29 June 2023

improve thermal performance. Usually, it was not possible to open the inner frame once the second frame was installed. In the second part of the nineteenth century, coupled windows (so-called box-windows) became common. Typically, box-windows include a secondary casement connected by hinges to the outer casement, making it possible to open for ventilation and maintenance. Many different variants of such window types exist, which are characteristic for the country/region and the decade of the building construction. In some designs, the two layers of sashes may open towards the inside or the outside; however, the essential idea is the same. Examples of buildings with a high number of original box-windows can be seen across Europe (Lorinczi, 2005). Nowadays, similar window concepts have received considerable research attention. In some designs, air can pass between the frames, where it is preheated from window heat losses or solar radiation. The air pathway depends on the operational mode and may be used for indoor ventilation or the airflow can be directed to the outside to lower solar heat gains, depending on the thermal requirements. Several studies describe those systems (Kang et al., 2017) (Zhang et al., 2016a) (Carlos, 2017) (Dalal et al., 2009) (Michaux et al., 2019) (Choi et al., 2019) (Lago et al., 2019); in some designs, shading systems were added for better control over solar gain (ZeyninejadMovassag and Zamzamian, 2020) (Zhang et al., 2016b).

Window attachments act as an additional layer that may improve glare and window insulation properties, influencing all three mechanisms of heat transfer.

- conductive: shade material/structure adds thermal resistance,
- convective: shade forms additional air space, which changes conditions for convection flows,
- radiative: shade material creates an additional barrier that changes conditions for radiative heat exchange (including influence on solar gains).

Currently, various window attachments are commonly used to provide glare protection, privacy and reduce solar gain. The ability of shades to effectively reduce heat gain has been proven in many investigations (Ye et al., 2016) (Her et al., 2016) (Alam and Islam, 2017) (Dutta et al., 2017). Venetian blinds have received a significant amount of research focus in this aspect (Fathoni et al., 2016) (Gomes et al., 2014) (Roeleveld et al., 2010) (Khamporn and Chaiyapinunt, 2014).

Shades are frequently integrated with automated controls that can adjust parameters for better solar gain control and comfort (Katsifaraki et al., 2017) (Fitton et al., 2017) (Tan et al., 2020) (van Moeseke et al., 2007). The same systems can assure shade in periods in which additional window insulation is desired. The presence of shading due to other reasons and availability of automated controls motivate further research in shading potential for improvements of thermal performance.

1.2. Former studies

This section looks at the extant research investigating shading influence solely on a window's thermal insulation properties. Window attachments are grouped depending on the installation location.

Shading placed on the outdoor side of the window. Historically, shutters were the first window attachments that provided privacy, safety and better thermal performance. Traditional shutters were replaced by external shades with many designs and different materials. Researchers have explored the performance of available solutions (Naylor et al., 2017) (Oleskowicz-Popiel and Sobczak, 2014) and also proposed new designs with focus on thermal performance (Gruner and Matusiak, 2018) (Shurcliff, 1980) (Langdon, 1980) (Soares et al., 2014). Results proved the potential for energy savings. However, external shading is usually not suitable due to its impact on the appearance of historic building facades.

Shading placed in between glazing. Most of the studies look at venetian blinds mounted in between panes of insulating glazing units (IGU). Huang et al. used the hot plate apparatus to define centre-of-glazing properties of IGU with an encapsulated venetian blind (Wright et al., 2008). The authors concluded that the U-value of the measured unit decreases while spacing between panes increases (tested distances from 15 to 40 mm). Best thermal improvements were achieved for blind slats set to low angles (shades nearly closed or fully closed). The effect of the temperature difference across the specimen showed a minor influence on the U-values. The second part of the study focused on formulating a calculation model describing venetian blind performance (Wright et al., 2008). Grynning et al. investigated experimentally using a hot-box apparatus with three insulated glazing units (2P, 3P and 4P) with integrated venetian blinds (Grynning et al., 2015). Measurements indicated minor reductions of U-values related to slat positions of the venetian blind (maximum 3% for vertical positions versus open position). Furthermore, the study concluded that shading presence in IGU lowers the thermal performance; thermal bridging of shading hardware was recognized to be the reason. The study is a good example of demonstrating the importance of complete-system testing to present product performance in practice. No studies were found focusing on shading placement between glass panes in wider air gaps than 40 mm.

Shading placed by the indoor side of the window. This was investigated both experimentally and numerically. Many publications focused on model development and its validation for estimating centre-of-glazing performance with various shading attachments installed on the indoor side of the room (Oleskowicz-Popiel and Sobczak, 2014) (Fang, 2001) (Oosthuizen et al., 2005) (Oosthuizen, 2011) (Shahid and Naylor, 2005) (Naylor et al., 2006) (Marjanovic et al., 2005) (Cuevas et al., 2010). Study results concluded that shading is a promising alternative for thermal improvement. Based on the mentioned studies, the following guidelines for improving system performance can be drawn.

- incorporate low-emissivity fabric on the shade surface facing the glass,
- install the shade 15–50 mm from the pane,
- restrict airflow between shade and glazing.

The analysed studies did not explore temperature changes on the window surface caused by shading introduction and the potential consequences.

The study presented by Wood et al. experimentally investigated adding insulation to relatively low-performing historic windows (Baker et al., 2009). A double-hung vertical sliding sash window was tested in a climate chamber with different improvement strategies. Since only heat flow meters were used for U-value assessments, the authors were not able to examine the thermal performance of the entire system. Results only looked at the centre-of-glass energy loss reductions. Heavy curtains achieved 39% reduction, reflective roller blinds 66% and honeycomb-type blinds 60% reduction. The base window was relatively low performing (single-pane glazing, thin wooden frame), thus reported improvements were relatively high. Influences of shading installation on condensation aspects were not discussed.

Besides market-available solutions, unconventional designs were created with a focus on energy performance. Hashemi et al. proposed a simple indoor shutter constructed with 50 mm thick Extruded Polystyrene (XPS) (Hashemi and Gage, 2014). The design was tested experimentally and numerically in various configurations. Energy use reduction was concluded to be over 60% for both assessment methods. Results showed that sealing air spaces between shade and window is important to reduce energy loss. Furthermore, experiments considered condensation risk under a range of environmental conditions. Condensation occurrence was dependent on the indoor air parameters, which in turn was very dependent on indoor conditions. The authors concluded that for the studied commercial space within regular space use, condensation did not occur until the temperature outside reached -5 °C. The same authors built a shutter with Vacuum Insulation Panels (VIP) and compared them against the shutter constructed with conventional

insulation materials using numerical simulation (Hashemi et al., 2019a). Despite using highly insulating VIPs (with 5.8 times lower conductivity than XPS), shade improvement was 84%, while shutters with convectional insulation achieved improvements of 79%. The authors concluded that relatively low performance of shades with VIPs was connected to thermal bridging occurring on the wall perimeter. After restricting the thermal bridging, the system achieved over 95% improvement. This shows the importance of planning system details to use all of the potential of highly insulating components. Airtightness and air cavity properties were not studied in detail.

The most recent study investigated the thermal bridging effect of VIP shutters, width of airspace between glass and shutter (50–200 mm) and application of trickle vents, allowing ventilation of the air space to the outside (Hashemi et al., 2019b). Results showed good thermal improvements and identified the thickness of airgap as an important parameter. Simulations indicated the best energy reductions for the thinnest airspace of 50 mm, which was assigned to a cold bridge occurring on the window recess perimeter.

Weinlaeder et al. applied phase change materials to the filling of slats in indoor vertical blinds (Weinlaeder et al., 2011) and tested their solar gain capabilities. The authors concluded that such a construction (even if slats were perpendicular to the glass surface) can contribute to the better thermal comfort of occupants in two ways: first by improving the temperature profiles between heating cycles and second by shading the cold window surface during the heating season. Lee et al. presented innovative roller-shade constructions of foil layers with small enclosed air volumes (called air caps) (Lee and Seo, 2018). The design was tested experimentally, in two configurations: fully deployed and deployed to half height of the window. The results demonstrated heating demand to be lower by 18.5% (for shade deployed to half height) and 33% (for fully deployed shade). Continuation of the study presented a more advanced design (Lee and Seo, 2018). Infiltration of the air gap between the glass surface and shade reduced with the detailed design. Aside from energy consumption for space conditioning, lighting energy was considered. Results showed increased energy consumption for lighting after shade installation; however, total energy demand was reduced by 26% in summer and 29% in winter. The study proved that even partially deployed shade leads to energy savings.

1.3. Aim, novelty and importance of presented study

The current study focuses on determining possible thermal improvements through shading attachments for box-windows. The thermal transmittance coefficient (U-value) was investigated for several configurations and compared against window base performance. Two different types of shades (roller and cellular shade) along with three placements (within the box-window and inside and outside the window recess) are considered. For aesthetic reasons, external shades/shutters were excluded from consideration. Ten configurations were experimentally tested in the hot-box apparatus (including two determining thermal performance of box-window without shading). Due to the possible use of the study results in heritage sites, focus was placed on condensation issues that may arise after shading installation. The following aims were set for the study.

- experimentally investigate the thermal performance of the box-window,
- explore shading construction and installation details which can result in further reduction of energy losses from box-windows,
- demonstrate the complete window and shade assembly which is closest to real-life performance,
- evaluate the influence of shading system installation on condensation risk, based on local temperature measurements.

The novelty and importance of the study can be summarized as follows.

- providing validated and straightforward thermal improvement options for box-windows is crucial. These windows are prevalent in many older buildings across Europe, and their replacement or structural retrofit may be infeasible due to regulations and cost constraints,
- since shading attachments are often added to windows for various reasons, presenting an overview of options, along with improvement indications, can be useful for practitioners,
- the study's experimental setup closely mimics real-life scenarios and includes installation details typical of shade installations. Additionally, the study accounts for airflows on the perimeter, which previous research has identified as an essential factor,
- unlike most previous studies that concentrate solely on the centre-of-glazing performance, this study's focus is on the entire product, taking into account all phenomena and estimating real-life performance more accurately,
- the study aimed to experimentally investigate the shade performance of shading systems installed in between glass panes with air gaps wider than 40 mm, which had not been previously explored according to available literature,
- the potential for condensation in various areas of the windows is considered, with introduction of various shading configurations,
- the results presented are valuable for validating simulations and calculation algorithms. They can also serve as a benchmark for future research in this area.

2. Methodology and experimental design

2.1. Specimen and test series overview

Window. The specimen used for testing was a typical box-window, where sashes were separated by a 120 mm wide air gap. The window was subdivided into six sections with two vertical and one horizontal divider. The frame facing towards the outside environment had fixed glazing except for the top central division which was fitted with an operable sash. In the inside frame, four panes were fitted in openable sashes and two others were fixed (the bottom right and bottom left). The entire window was glazed with 4 mm thick uncoated glass (as is typical for most of the original box-window designs). The two fixed glass units on the indoor frame were held in place by wooden glazing beads, while the other glass was fitted into 8–11 mm grooves and traditionally secured with metal nails and sealed with linseed oil-based putty. The sashes were held with traditional small hinges and simple hardware with metal handles. The complete unit was 2200 × 2050 mm (width x

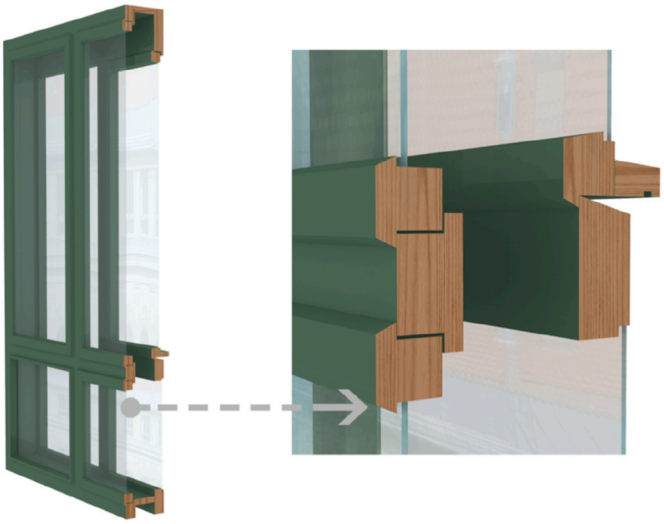

Fig. 1. A vertical cross-section of the tested box-window.

height). The unit was newly constructed and well protected against draughts (with seals) and considered airtight. Fig. 1 presents the cross-section of the window (with vertical symmetry plane to the right). During the testing, window sashes remained closed.

Shade placement. The box-windows in Central and Northern Europe were usually inserted in thick masonry wall constructions, typically 150–300 mm thick. In most cases, the window was installed towards the outdoor environment to protect against water intrusion. This creates a window recess on the indoor side of the window, which is typically over 70 mm deep. Such an arrangement allows shade installation in two places: **inside the window recess** and on the surface of the wall surface surrounding the window opening (referred to later as a position **outside the window recess**). To model the window recess, an additional wooden frame was built with wooden furring strips (23 × 98 mm) around the perimeter of the tested window. This created a 98 mm deep window recess in which shades were positioned in middle-distance to the glass, i.e. 45 mm. Closer positions were not possible since the sash hardware handles obstructed the shade operation. For shade installation outside the recess, the closest distance to the wall was kept, at the same time allowing for shade operation (20 mm).

Another possible placement was considered between window sashes, referred to later in the study as a position **within the box-window**. Due to thermal and practical aspects, a symmetrical position between glass panes (60 mm) of the shades was chosen. See Fig. 2 for possible installation placements.

Shades. Two different shade types were chosen for the testing.

Cellular shades – so-called "honeycomb shades" – were introduced to the market relatively recently. Honeycomb shades are advertised as a type of "thermal shade" due to their structure of small air gaps which are supposed to generate additional thermal resistance. There are several variations of honeycomb shades. Fig. 3 presents some designs available on the market. For the experiment, the cell-in-cell shade solely made of fabric was chosen (item D in Fig. 3). The tested shade had an electric motor and controller allowing for remote operation.

Roller-shades are commonly used due to their simplicity and relatively low price. As well as the basic roller-shade design (Fig. 4A), there are also market-available solutions including side guides and cassettes for rolled fabric (Fig. 4B). These restrict airflow between the indoor environment and the created gap (between shade and glass) which may increase thermal resistance. Initially, a basic market-available product was chosen, i.e. mechanically operated roller-shade (without guides and cassette) with fabric made of polyester. In some cases, thin wooden guides were created for the sides, bottom and top of the shade to restrict airflow. Another modification was lowering the fabric emissivity on the surface facing the outdoor environment which was achieved by gluing (with double-sided tape) aluminium foil on the shade's surface. This configuration is later referred to as the reflective roller-shade.

Test series. Altogether ten configurations of box-window and shading were investigated. Table 1 presents the case description while Fig. 5 illustrates simple sketches of the tested configurations. The base performance of the window was established for both configurations with and without recess since a recess changes airflow patterns close to the specimen's warm side.

2.2. Test procedure and instrumentation

Hot-box apparatus. Measurements were carried out in a guarded hot-box apparatus (Fig. 6A) according to procedures described in ISO 8990 (EN ISO 8990, 1996) and ISO 12567–1 (International Organization for Standardization, 2010), what would be a typical methodology for thermal assessment of a window specimen.

The tests were performed in steady-state conditions. Temperatures were set to +20 °C on the warm side and 0 °C on the cold side (typical U-value test conditions).

Window U-values are based on the measured heat flows, surrounding temperatures and window area as shown in Eq. (1). The U-value given is the mean value of 24 1-h-long measurement periods (the data sampling rate is every 10 s).

$$U_w = \frac{\Phi_w}{A_w \cdot \Delta\theta_{ie}} = \frac{\Phi_{IN} - \Phi_{sur} - \Phi_{EXTR} - \Phi_{FL,W}}{A_{W \cdot \Delta\theta_{ie}}} \quad \text{Eq. (1)}$$

where.

U_W = window U-value (W/(m^{2}K))
A_W = window area (m^2)
θ_{ie} = temperature difference over sample (K)
Φ_{IN} = power input to metering chamber (W)
Φ_{sur} = surrounding panel heat flow (W)
Φ_{EXTR} = metering chamber wall heat flow (W)
$\Phi_{FL,w}$ = test sample flanking heat loss (W)

The window was mounted in a template constructed as a 198 mm thick wood-frame construction clad with 8 mm plywood on the faces exposed to the hot and cold sides. The joints between the window and the surround panel were sealed with tape on both sides to ensure an airtight seal. Minor gaps between window frame and template were filled with Expanded Polystyrene (EPS).

The metering area of the hot-box was 2.45 m × 2.45 m. The window was placed in the middle of the metering area template wall at a distance of 0.1 m from the lower edge of the metering area.

The external surface thermal resistance coefficient was adjusted close to the standardized value, R_{se} = 0.04 W/(m^{2}K), prior to the tests by

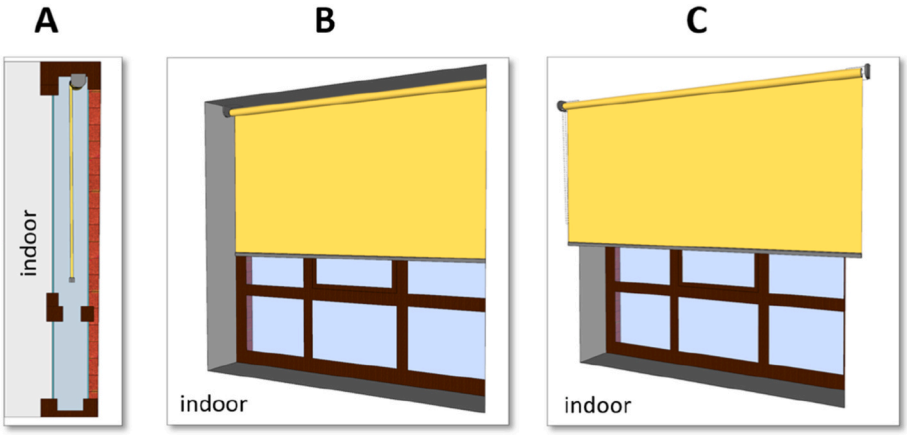

Fig. 2. Considered shade placements: A – shade within the box-window, B – shade inside the window recess, C – shade outside the window recess. (For interpretation of the references to colour in this figure legend, the reader is referred to the Web version of this article.)

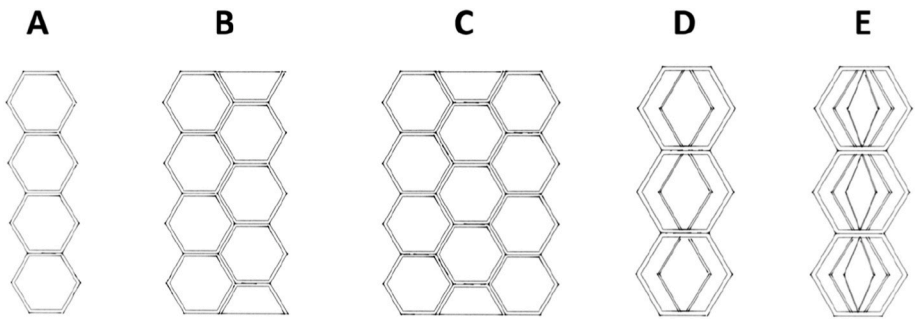

Fig. 3. Cross-sections of different types of cellular shades available on the market. A – one row, B – two rows, C – three rows, D – cell-in-cell, E – cell-in-cell+. The internal surfaces may be lined with a thin aluminium layer to lower the intensity of heat transfer through radiation.

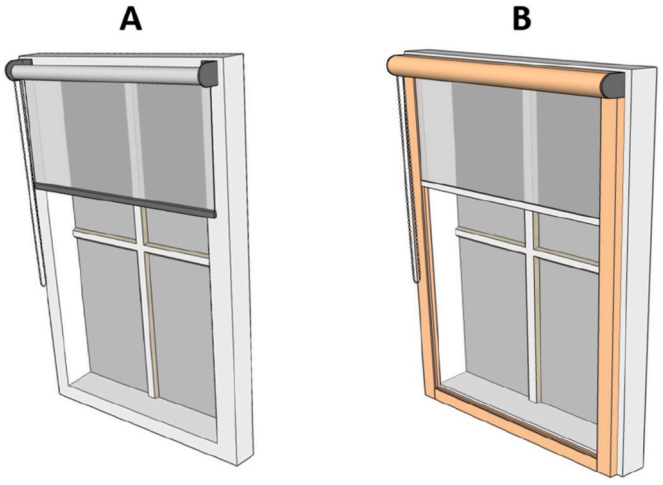

Fig. 4. A – basic roller-shade type used in the study, B – roller-shade design with guides on the side and top cassette for rolled shade. (For interpretation of the references to colour in this figure legend, the reader is referred to the Web version of this article.)

calibration of airflow velocities adjacent to the template surface on the cold side. Natural convection-driven airflow was maintained on the warm side to give a thermal resistance coefficient very close to the ISO 8990 standard value of R_{si} = 0.13 W/(m^{2}K). However, during the measurements, the surface thermal resistances may differ slightly from the standardized values. Corrections to the values are made for these deviations so that all U-values are stated with normalized surface thermal resistance coefficients as specified in ISO 8990.

A calibration measurement to establish the overall thermal resistance of the wood-frame panel surrounding the test specimens was completed according to the procedure in ISO 12567–1. The window opening of the template was filled with EPS with the same thickness as the window frame depth (176 mm). The calibration measurement was carried out using the same temperature set-points for the cold and warm side of the hot-box as during the window measurements. The thermal resistance found through the calibration was used to calculate the surround panel heat flow, Φ_{sur}, during measurements of the window.

Additional temperature sensors. To assess possible risks of moisture condensation and future validation of numerical investigation, additional temperature sensors were introduced (see Fig. 6B for the location of these sensors). All sensors were placed in the vertical symmetry plane of the window. Horizontal sensors 291, 286, 283, 284, 276, 272 and 271 were placed in the middle of the upper glass pane; sensors 281 and 273 were placed three-quarters up the upper pane. Sensors 293, 282, 277 and 278 were placed at the divider level. Sensors 297, 287, 272 and 275 were placed at the symmetry axis of the lower pane. Sensors 296, 285, 279 and 290 were located at the frame connection level with the lower pane. Sensors 299 and 289 were placed 25 mm above the connection, and sensors 298 and 288 were placed 50 mm above the connection.

Uncertainty assessments of hot-box measurements. The uncertainties associated with the hot-box measurements were assessed in accordance with the procedure described in ISO 12567–1. The total uncertainty propagation of the measured U-value, $\Delta^P U_w/U_w$, was derived using the root-mean-square method as shown in Eq. (2).

$$\frac{\Delta^P U_w}{U_w} = \sqrt{\left[\frac{\Delta^P \Phi_w}{\Phi_w}\right]^2 + \left[\frac{\Delta^P A_w}{A_w}\right]^2 + \left[\frac{\Delta^P \delta\theta_{ie}}{\theta_{ie}}\right]^2} \quad \text{Eq. (2)}$$

where,

$\Delta^P\Phi_w/\Phi_w$ = uncertainty in sample heat flow (W)
$\Delta^P A_w/A_w$ = uncertainty of projected area of sample (m^2)
$\Delta^P\delta\theta_{ie}/\delta\theta_{ie}$ = uncertainty in temperature difference between warm and cold side (K)

The uncertainty in the sample heat flow is based on the heat balance equation for the metering chamber. The uncertainty in the test sample specimen heat flow, $\Delta^P\Phi_w/\Phi_w$, is expressed using Eq. (3).

$$\frac{\Delta^P \Phi_w}{\Phi_w} = \sqrt{\left(\frac{\Delta^P \Phi_{IN}}{\Phi_w}\right)^2 + \left(\frac{\Delta^P \Phi_{sur}}{\Phi_w}\right)^2 + \left(\frac{\Delta^P \Phi_{EXTR}}{\Phi_w}\right)^2 + \left(\frac{\Delta^P \Phi_{FL,w}}{\Phi_w}\right)^2} \quad \text{Eq. (3)}$$

where,

$\Delta^P\Phi_{IN}$ = uncertainty in power input to metering chamber (W)
$\Delta^P\Phi_{sur}$ = uncertainty in surrounding panel heat flow (W)
$\Delta^P\Phi_{EXTR}$ = uncertainty in metering chamber wall heat flow (W)
$\Delta^P\Phi_{FL,w}$ = uncertainty in test sample flanking heat loss (W)

No correlation between the various terms of the balance equation was found. A calibration experiment for the thermocouples was carried out using a reference temperature bath. The relative scattering in measured temperatures between the thermocouples was found to be lower than 0.02 °C. Thus, it can be concluded that the influence from factor $\Delta^P\delta\theta_{ie}$ as described in Eq. (2) is negligible. The areas of the windows ($\Delta^P A_w$) were measured with an accuracy of ±0.5 mm and can thus be concluded to be negligible compared to the uncertainty of the $\Delta^P\Phi_w/\Phi_w$ term in Eq. (2).

The uncertainties stated in this work are given with a coverage factor of two standard deviations and the corresponding 95% confidence interval.

3. Results

The results of the measurements are presented in Table 2. For each case described in the table, the following values are reported.

Table 1
Test series description.

No	Label/name	Comments
1.	Base window performance (no window recess added)	Investigating window base performance. Cellular shade is symmetrically located between the indoor and the outdoor window frame and remains fully retracted during the test.
2.	Cellular shade within the box-window (no window recess added)	The shade stays in the same place as for case 1 and is fully deployed. Distance from frame to shade perimeter (except for the top of the shade, where shade is installed tight to the window frame) is around 15 mm to provide the distance for proper shade operation.
3A.	Base window performance (window recess added on the indoor side) (shade installed inside the window recess)	Investigating window base performance including window recess added on the warm side of the specimen. During the test, cellular shade is installed inside the window recess and remains in a fully retracted position.
3B.	Base window performance (window recess added on the indoor side) (shade installed outside window recess)	Investigating window base performance including window recess added on the warm side of the specimen. During the test, cellular shade is installed outside the window recess and remains in a fully retracted position.
4.	Cellular shade inside the window recess	Cellular shade installed inside window recess with 50 mm distance to the glass surface. The distance between perimeter and recess surface is around 10 mm (except for the top of the shade, where shade is tightly installed to upper recess surface).
5.	Cellular shade outside the window recess	Shade distance from shade to the glass surface is set to 120 mm, while shade distance from the most indoor surface of the window recess is around 20 mm.
6.	Roller-shade within the box-window	Shade located symmetrically between glass panes. The distance between shade perimeter and the window frame is set to about 10 mm.
7.	Reflective roller-shade within the box-window	Shade located in the same manner as for case 6. Low-emissivity surface of shade facing the outdoor environment.
8.	Reflective roller-shade inside the window recess	Shade located inside the window recess; the distance between shade and glass surface is set to 50 mm. The distance between shade perimeter and recess surface is 10 mm.
9.	Reflective roller-shade inside the window recess with restricted air on perimeter	Testing setup remains the same as for case number 8. Airflows on perimeter are limited by wooden guides (20 × 12 mm) installed on the sides, bottom and top. The setup allows some air to migrate in the space between shade and window due to narrow gaps created by freely hanging shade material.
10.	Reflective roller-shade outside the window recess	Shade is installed outside the window recess to simulate shade placement on the wall surface. Distance from shade surface to the window is kept at 120 mm while the distance between shade perimeter and the most indoor surface of window recess is set to 20 mm.

- $\mathbf{U_{value}}$ – measured U-value of the complete system (W/m^{2}K), including uncertainties calculated according to Eq. (2),
- $\mathbf{\%\ U_{value}}$ – improvement in percentage in relation to the base window without shade (%),
- $\mathbf{T_{indoor}}$ – the lowest temperature on the indoor surface of the window (^{o}C),
- $\mathbf{d\ T_{indoor}}$ – change of T_{indoor} in relation to the base window (^{o}C),
- $\mathbf{T_{inside}}$ – the lowest temperature measured inside the box-window (^{o}C), $\mathbf{d\ T_{inside}}$ – change of T_{inside} in relation to the base case of the window without shade (^{o}C).
- $\mathbf{TS_{number}}$ – Temperature Sensor readings (271–299), for the sensor location please refer to Fig. 6.

Percentage improvements of the U-value and lowest temperatures are related in the following way: for cases 2, 6 and 7, the mentioned values are related to the performance of the base window without recess (case 1), for cases 4, 8 and 9 to case 3A, and remaining cases to case 3B. The lowest temperatures on the indoor surface and inside the box-window were found at sensors 299 and 288 (refer to Fig. 6B) for all of the cases.

4. Discussion

As highlighted in the introduction, shades may be able to improve the thermal performance of windows by influencing each of the heat transfer mechanism i.e., conduction, convection, and radiation. The study results demonstrate that all of the shading configurations proposed in this research lead to a reduction in heat losses from the box-window.

The highest thermal performance improvement, which is around 46%, was achieved by using the reflective roller-shade along with wooden guides (which restrict airflows on perimeters), installed inside the window recess (case 9). The measured U-value of this configuration is reduced from 1.91 W/m^{2}K (case 3A, window with retracted shade) to 1.03 W/m^{2}K (case 9, window with shade deployed). Due to low thickness of the roller-shade, reduction of conductive heat transfer may play minor role. The majority of the reduction in heat losses observed can be attributed to the creation of an additional air gap and the reflective properties of the shading material. Comparing case 9, which resulted in 32% greater improvement, to case 8 (the same shade, without guides constraining airflows) we can draw conclusion that guides restricting airflows have a significant role in this case.

However, for the case 9, the temperature on the indoor window surface dropped by 6 °C and reached a temperature of 5 °C (the outdoor temperature was set to 0 °C). Since the space between window and shade was not airtight, air containing moisture can migrate or be trapped when the shade is deployed. The presence of indoor air in the vicinity to a cold window surface may result in moisture condensation, what may exclude this option in certain cases.

Simple roller-shade without any modification installed inside the box-window (Case 6) demonstrated visible U-value improvements by 19%. Similarly, as previously observed for roller shades, their limited thickness results in a small impact on conduction heat transfer. The improvement of insulation could be attributed to the creation of two smaller air gaps, resulting in two separate conduction loops that enhance thermal resistance. Additionally, the introduction of an extra layer reduces radiative heat transfer by dividing the heat exchange mechanism into smaller portions, leading to lower heat losses. Radiation effect is clearly visible in case 7, where an aluminium foil-coated shade, showing 80% greater improvements in heat insulation than a basic roller-shade in the same placement (case 6), thus shade surface emissivity plays important role.

Cellular shades proved that their design/structure provides some additional thermal resistance. Comparison of cases 2 and 6 indicates that cellular shade in the same placement delivers 42% higher reductions in comparison to the roller-shade. The fabric of the roller-shade itself provides negligible thermal resistance due to its limited thickness. Cellular shade is structured in the way that fabric splits the air space into smaller gaps, which changes convection loops, thus improving the insulation properties of the window. Use of other variations of cellular

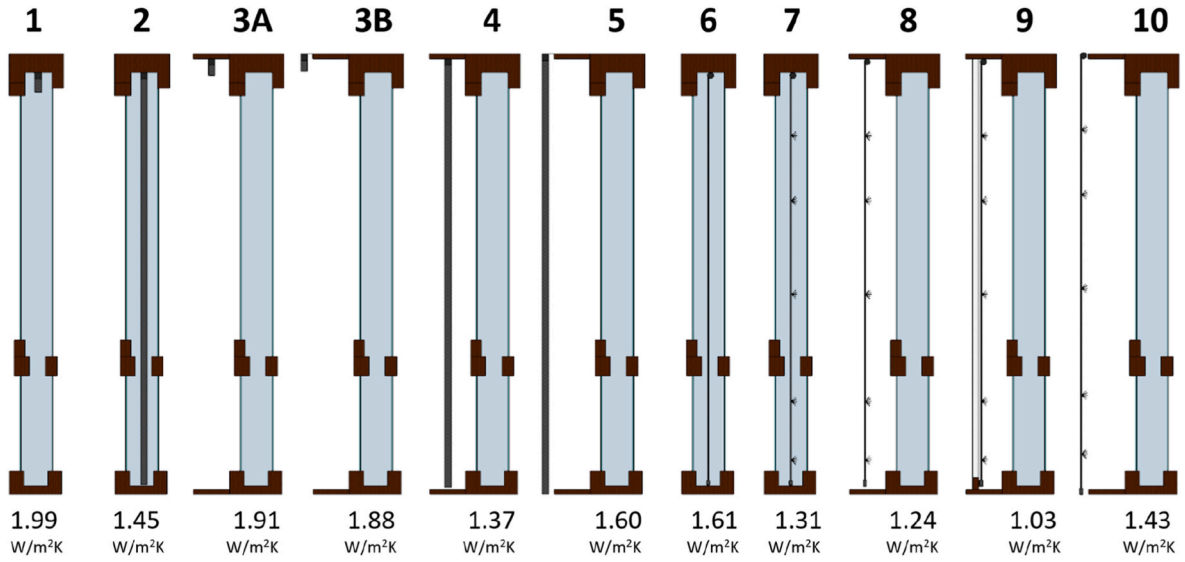

Fig. 5. Configuration sketches, along with numbers that correspond to Table 1. Cases 7–10 include low-emissivity surface covering the shade fabric marked with small lines perpendicular to shade surface. Below each case the measured U-value is presented. (For interpretation of the references to colour in this figure legend, the reader is referred to the Web version of this article.)

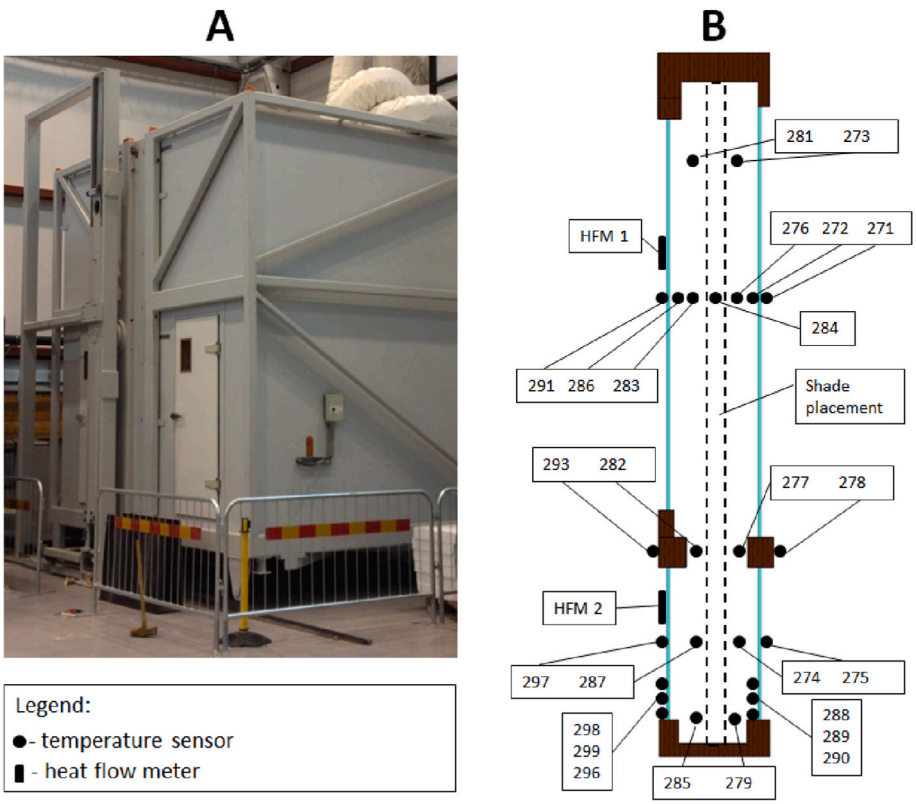

Fig. 6. A – the large-scale guarded hot-box test facility used for the measurements.
B – additional temperature sensors added for the measurements. The placement of sensor number 284 varies with the setup. For cellular shades, it is located on the fabric splitting the air cavities inside the shade, while for roller-shades it is located on the shade surface facing the outdoor environment. (For interpretation of the references to colour in this figure legend, the reader is referred to the Web version of this article.)

shades, including more rows and an additional low-emissivity layer (see examples presented in Fig. 3), may result in further improvements. Additional enhancements may be achieved by using guides to restrict air on the shade perimeter but this was not tested in this study.

Comparing shading placements for the same configuration of cellular shades (cases 2, 4, 5) and roller-shades (case 7, 8, 10) indicates that most favourable placements in terms of boosting window insulation are achieved both by placement inside the box-window and inside the window recess. Placement outside the window recess gives lower improvements than the two other shade locations, probably due to higher air exchange in the cavity between shade and window.

If the prevention of condensation is a priority concern, then the optimal position for the shading would be inside the box-window. This placement results in lowering the risk of condensation on indoor surfaces of the window since it slightly raises its temperature (by 1 °C). However, the introduction of the shading inside the box-window lowers the temperature on the most outer glass. For the testing conditions, the temperature dropped from 1 °C to 0 °C. However, condensation risk due

Table 2
Measurement results.

Case	1	2	3A	3B	4	5	6	7	8	9	10
U_{value} ± ΔPUw/ Uw	1.99 ± 0.03	1.45 ± 0.02	1.91 ± 0.02	1.88 ± 0.01	1.37 ± 0.02	1.60 ± 0.02	1.61 ± 0.02	1.31 ± 0.02	1.24 ± 0.02	1.03 ± 0.02	1.43 ± 0.02
% U_{value}	n/a	27	n/a	n/a	28	16	19	34	35	46	25
T_{indoor}	11.49	12.06	11.21	11.14	7.31	9.36	12.18	12.11	7.08	5.25	8.28
d T_{indoor}	n/a	0.6	n/a	n/a	−3.9	−1.9	0.7	0.6	−4.1	−6.0	−2.9
T_{inside}	1.19	0.00	1.10	1.04	0.00	0.00	0.00	0.00	0.00	0.00	0.00
d T_{inside}	n/a	−1.2	n/a	n/a	−1.1	−1.1	−1.2	−1.2	−1.1	−1.1	−1.1
TS 271	1.74	1.10	1.61	1.53	0.00	1.27	1.22	0.00	0.00	0.00	1.12
TS 272	2.76	1.85	2.77	2.67	1.86	2.26	2.30	1.73	1.73	1.38	2.00
TS 273	10.63	10.10	10.36	10.04	8.33	9.23	10.60	11.36	7.58	6.74	8.56
TS 274	5.28	3.18	5.03	4.93	3.24	4.11	4.41	4.42	3.13	2.35	3.69
TS 275	2.00	0.00	1.88	1.82	1.06	1.46	1.08	0.00	1.06	0.00	1.32
TS 276	8.05	7.07	7.72	7.60	5.71	6.67	7.49	8.35	5.34	4.36	5.99
TS 277	5.95	4.30	5.77	5.61	3.98	4.78	3.88	5.08	3.75	2.92	4.29
TS 278	0.00	0.00	0.00	0.00	0.00	0.00	0.00	0.00	0.00	0.00	0.00
TS 279	4.20	2.67	4.00	3.92	2.58	3.29	3.56	3.40	2.51	1.90	2.97
TS 281	10.65	13.37	10.36	10.00	8.38	9.28	11.49	13.95	7.61	6.79	8.57
TS 282	6.55	9.00	6.20	6.05	4.33	5.16	7.80	8.11	4.04	3.20	4.64
TS 283	8.15	10.81	7.84	7.73	5.81	6.77	9.48	11.55	5.46	4.48	6.12
TS 284	12.88	9.57	11.79	11.65	10.89	11.23	13.11	15.38	10.18	9.50	11.00
TS 285	4.88	4.77	4.68	4.61	3.19	3.93	4.56	5.10	3.11	2.41	3.58
TS 286	12.57	15.06	12.29	12.13	8.92	10.35	14.15	15.69	8.38	6.91	9.37
TS 287	5.35	6.75	5.14	5.05	3.35	4.21	5.90	6.99	3.24	2.47	3.80
TS 288	1.19	0.00	1.10	1.04	0.00	0.00	0.00	0.00	0.00	0.00	0.00
TS 289	1.29	0.00	1.18	1.11	0.00	0.00	0.00	0.00	0.00	0.00	0.00
TS 290	1.65	0.00	1.54	1.47	0.00	1.22	0.00	0.00	0.00	0.00	1.12
TS 291	13.90	15.96	13.64	13.47	9.88	11.47	15.22	16.49	9.36	7.72	10.44
TS 293	15.39	16.33	14.85	14.69	10.55	12.24	15.97	16.51	9.26	7.68	10.86
TS 296	12.24	12.77	12.00	11.89	7.61	9.88	12.84	12.97	7.40	5.38	8.69
TS 297	12.70	13.64	12.39	12.44	7.86	10.23	13.69	14.38	7.91	5.96	9.44
TS 298	11.81	11.66	11.50	11.79	7.61	9.90	12.44	12.52	7.64	5.61	8.97
TS 299	11.49	12.06	11.21	11.14	7.31	9.36	12.18	12.11	7.08	5.25	8.28

to lower temperatures on the outer frame of a box-window may be easier to eliminate. Firstly, draught-proofing of the frame facing indoors may reduce indoor air migration to the space between windows. Secondly, providing small ventilation gaps in the outer frame may help to ventilate space outside. Homb and Uvsløkk reported that in a similar setup, removal of small pieces of seal from the outer frame improves the self-drying process of the space between the frame, and eliminates condensation and at the same time limits the decrease in thermal performance (Homb and Uvsløkk, 2012).

When shades are installed inside the window recess, the problem of condensation may be more difficult to mitigate. Even the introduction of side guides may not be sufficient to prevent condensation, as during the deployment of the shade, air with high relative humidity may become trapped in between the shade and the window surface. Moisture contained in the air will condense on the colder areas of the window, potentially leading to issues with moisture damage or mold growth.

5. Conclusions and further work

The conducted measurements proved that shading installed along with the original box-window has a positive impact on the window thermal performance. The highest U-value reduction by 46% was achieved by the roller-shade installed inside the window recess, including a low-emissivity layer on its surface and wooden guides constraining airflow on the shade perimeter. For this shade configuration, the U-value was reduced from 1.91 to 1.03 W/m^{2}K. Combining experience gained in this research with other market-available shade solutions may result in further improvements. A cellular shade with a higher number of rows/cells including low-emissivity layers seems to be promising. Restricting airflow on the shading perimeter was identified as being important.

The analysis showed that the higher potential risk of condensation on the indoor surface of the window is caused by shade placed on the indoor side of the window. For the most extreme case, the temperature dropped by 6 °C and reached a temperature of 5 °C, while the outside temperature was set at 0 °C. Such a low temperature carries a high condensation risk which may affect the window's durability and indoor climate.

It was concluded that placement within the box-window is the most favourable since it does not increase the risk of condensation on indoor window surfaces while providing good thermal improvements. Possible condensation inside the box-window may be lowered by draught-proofing the indoor frame and providing ventilation towards the outside environment between the glass.

Shades proved to be an effective solution for improving the thermal properties of box-windows. Shade installation is often motivated by other reasons; it is therefore worth considering the findings of this work to improve the thermal performance of the window. While assessing shading installation, it is important to consider condensation risk depending on the shade location and temperature/moisture conditions of the indoor environment.

Further work should focus on developing models/establishing routines for modelling box-windows along with shading attachments. The presented data may be helpful with the validation process. Further investigations including cellular shades along with installation alternatives should be conducted to provide cost-effective energy retrofit of box-windows as an alternative to structural changes or replacement of original box-windows.

Declaration of competing interest

The authors declare the following financial interests/personal relationships which may be considered as potential competing interests: Cezary Misiopecki reports financial support was provided by the Research Council of Norway, Lian Vinduer AS, Lawrence Berkeley National Laboratory (LBNL), and EU FP7 EFFESUS.

Data availability

Main data used in the studies are included in the paper.

Acknowledgments

This work has been funded by the Research Council of Norway, Lian Trevarefabrikk and Lawrence Berkeley National Laboratory (LBNL) through the research project "Improved Window Technologies for Energy Efficient Buildings" (EffWin), and through the EU FP7 EFFESUS project (www.effesus.eu).

References

Alam, M.J., Islam, M.A., 2017. Effect of external shading and window glazing on energy consumption of buildings in Bangladesh. Adv. Build. Energy Res. 11, 180–192. https://doi.org/10.1080/17512549.2016.1190788.

Baker, P., Wood, C., Bordass, B., 2009. Research into the thermal performance of traditional windows: timber sash windows English heritage. https://research.historicengland.org.uk/Report.aspx?i=16035.

Bertone, E., Sahin, O., Stewart, R.A., Zou, P., Alam, M., Blair, E., 2016. State-of-the-art review revealing a roadmap for public building water and energy efficiency retrofit projects. Int. J. Sustain. Built Environ. 5, 526–548. https://doi.org/10.1016/j.ijsbe.2016.09.004.

Carlos, J.S., 2017. Optimizing the ventilated double window for solar collection. Sol. Energy 150, 454–462. https://doi.org/10.1016/j.solener.2017.04.063.

Choi, H., An, Y., Kang, K., Yoon, S., Kim, T., 2019. Cooling energy performance and thermal characteristics of a naturally ventilated slim double-skin window. Appl. Therm. Eng. 160, 114. https://doi.org/10.1016/j.applthermaleng.2019.114113, 113.

Cuevas, C., Fissore, A., Fonseca, N., 2010. Natural convection at an indoor glazing surface with different window blinds. Energy Build. 42, 1685–1691. https://doi.org/10.1016/j.enbuild.2010.05.003.

Dalal, R., Naylor, D., Roeleveld, D., 2009. A CFD study of convection in a double glazed window with an enclosed pleated blind. Energy Build. 41, 1256–1262. https://doi.org/10.1016/j.enbuild.2009.07.024.

Dol, K., Haffner, M., 2010. Housing Statistics in the European Union. Ministry of the Interior and Kingdom Relations, The Hague.

Dutta, A., Samanta, A., Neogi, S., 2017. Influence of orientation and the impact of external window shading on building thermal performance in tropical climate. Energy Build. 139, 680–689. https://doi.org/10.1016/j.enbuild.2017.01.018.

EN ISO 8990, 1996. ISO 8990 Thermal Insulation – Determination of Steady-State Thermal Transmission Properties – Calibrated and Guarded Hot Box. Bsi, p. 26, 1994. https://www.iso.org/standard/16519.html.

Fang, X., 2001. Study of the U-factor of a window with a cloth curtain. Appl. Therm. Eng. 21, 549–558. https://doi.org/10.1016/S1359-4311(00)00071-5.

Fathoni, A.M., Chaiwiwatworakul, P., Mettanant, V., 2016. Energy analysis of the daylighting from a double-pane glazed window with enclosed horizontal slats in the tropics. Energy Build. 128, 413–430. https://doi.org/10.1016/j.enbuild.2016.06.034.

Fitton, R., Swan, W., Hughes, T., Benjaber, M., 2017. The thermal performance of window coverings in a whole house test facility with single-glazed sash windows. Energy Effic 10, 1419–1431. https://doi.org/10.1007/s12053-017-9529-0.

Gomes, M.G., Santos, A.J., Rodrigues, A.M., 2014. Solar and visible optical properties of glazing systems with Venetian blinds: numerical, experimental and blind control study. Build. Environ. 71, 47–59. https://doi.org/10.1016/j.buildenv.2013.09.003.

Gray, V., 2007. Climate change 2007: the physical science basis summary for policymakers. Energy Environ. 18, 433–440. https://doi.org/10.1260/095830507781076194.

Gruner, M., Matusiak, B.S., 2018. A novel dynamic insulation system for windows. Sustain. Times 10. https://doi.org/10.3390/su10082907.

Grynning, S., Misiopecki, C., Gustavsen, A., 2015. Thermal performance of in-between shading systems in multilayer glazing units: hot-box measurements and numerical simulations. J. Build. Phys. 39, 147–169. https://doi.org/10.1177/1744259114559924.

Gustavsen, A., Arasteh, D., Jelle, B.P., Curcija, C., Kohler, C., 2008. Developing low-conductance window frames: capabilities and limitations of current window heat transfer design tools – state-of-the-art review. J. Build. Phys. 32, 131–153. https://doi.org/10.1177/1744259108097672.

Hashemi, A., Gage, S., 2014. Technical issues that affect the use of retrofit panel thermal shutters in commercial buildings. Build. Serv. Eng. Technol. 35, 6–22. https://doi.org/10.1177/0143624412462906.

Hashemi, A., Alam, M., Ip, K., 2019a. Comparative performance analysis of vacuum insulation panels in thermal window shutters. Energy Proc. 157, 837–843. https://doi.org/10.1016/j.egypro.2018.11.249.

Hashemi, A., Alam, M., Mohareb, E., 2019b. Thermal performance of vacuum insulated window shutter systems. In: (Accepted/In Press) Zero Energy Mass Custom Home (ZEMCH 2019) International Conference.

Her, J., Lee, H., Kim, Y., 2016. A preliminary study on the performance evaluation of a window according to the attachment position of insulation air cap in winter season. Adv. Sci. Technol. Lett. 124, 10–14.

Homb, A., Uvsløkk, S., 2012. Energy Efficient Windows with Cultural Value, Report 3D1110, SINTEF Building and Infrastructure, Materials and Structures.

International Energy Agency, 2013. Transition to sustainable buildings: strategies and opportunities to 2050. OECD 9789264202, 1–284. https://doi.org/10.1787/9789264202955-en.

International Organization for Standardization, 2010. Windows and Doors – Determination of Thermal Transmittance by the Hot-Box Method – Part 1: Complete Windows and Doors. ISO 12567-1:2010 Thermal performance of.

Kang, J.S., Oh, E.J., Bae, M.J., Song, D.S., 2017. A numerical study of the thermal characteristics of an air cavity formed by window sashes in a double window. Int. J. Thermophys. 38, 1–15. https://doi.org/10.1007/s10765-017-2309-4.

Katsifaraki, A., Bueno, B., Kuhn, T.E., 2017. A daylight optimized simulation-based shading controller for Venetian blinds. Build. Environ. 126, 207–220. https://doi.org/10.1016/j.buildenv.2017.10.003.

Khamporn, N., Chaiyapinunt, S., 2014. Effect of installing a Venetian blind to a glass window on human thermal comfort. Build. Environ. 82, 713–725. https://doi.org/10.1016/j.buildenv.2014.10.022.

Lago, T.G.S., Ismail, K.A.R., Lino, F.A.M., 2019. Ventilated double glass window with reflective film: modeling and assessment of performance. Sol. Energy 185, 72–88. https://doi.org/10.1016/j.solener.2019.04.047.

Langdon, W.K., 1980. Movable Insulation. A Guide to Reducing Heating and Cooling Losses through the Windows in Your Home. Rodale Press, Emmaus, PA, United States. https://www.osti.gov/biblio/6586566.

Lee, H., Seo, J., 2018. Development of window-mounted air cap roller module. Energies 11. https://doi.org/10.3390/en11071909.

Lorinczi, Z., 2005. Windows in Historical Hungary, 963 218 4750.

Marjanovic, L., Cook, M., Hanby, V., Rees, S., 2005. CFD modelling of convective heat transfer from a window with adjacent Venetian blinds. IBPSA 2005 – Int. Build. Perform. Simul. Assoc. 2005, 709–716.

Mazzarella, L., 2015. Energy retrofit of historic and existing buildings. The legislative and regulatory point of view. Energy Build. 95, 23–31. https://doi.org/10.1016/j.enbuild.2014.10.073.

Michaux, G., Greffet, R., Salagnac, P., Ridoret, J.B., 2019. Modelling of an airflow window and numerical investigation of its thermal performances by comparison to conventional double and triple-glazed windows. Appl. Energy 242, 27–45. https://doi.org/10.1016/j.apenergy.2019.03.029.

Naylor, D., Shahid, H., Harrison, S.J., Oosthuizen, P.H., 2006. A simplified method for modelling the effect of blinds on window thermal performance. Int. J. Energy Res. 30, 471–488. https://doi.org/10.1002/er.1162.

Naylor, D., Foroushani, S.S.M., Zalcman, D., 2017. Free convection heat transfer from a window glazing with an insect screen. Energy Build. 138, 206–214. https://doi.org/10.1016/j.enbuild.2016.11.062.

Oleskowicz-Popiel, C., Sobczak, M., 2014. Effect of the roller blinds on heat losses through a double-glazing window during heating season in Central Europe. Energy Build. 73, 48–58. https://doi.org/10.1016/j.enbuild.2013.12.032.

Oliveira, R.A.F., Lopes, J., Sousa, H., Abreu, M.I., 2017. A system for the management of old building retrofit projects in historical centres: the case of Portugal. Int. J. Strat. Property Manag. 21, 199–211. https://doi.org/10.3846/1648715X.2016.1251984.

Oosthuizen, P.H., 2011. Three-dimensional effects on convective heat transfer from a window/plane blind system. Heat Tran. Eng. 29, 565–571. https://doi.org/10.1080/01457630801893157.

Oosthuizen, P.H., Sun, L., Harrison, S.J., Naylor, D., Collins, M., 2005. The effect of coverings on heat transfer from a window to a room. Heat Tran. Eng. 26, 47–65. https://doi.org/10.1080/01457630590927345.

Roeleveld, D., Naylor, D., Oosthuizen, P., 2010. A simplified model of heat transfer at an indoor window glazing surface with a Venetian blind. J. Build. Perform. Simul. 3, 121–128. https://doi.org/10.1080/19401490903528147.

Schwehr, P., Fischer, R., Geier, S., 2011. Retrofit strategies design guide: advanced retrofit strategies & 10 steps to a prefab module. http://www.empa-ren.ch/A50/Annex 50 Final Publications for Internet/DesignGuide_ECBCS_A50.pdf.

Sedovic, W., Gotthelf, J.H., 2005. What replacement windows can't replace: the real cost of removing historic windows. APT Bull. J. Preserv. Technol. 36, 25–29.

Shahid, H., Naylor, D., 2005. Energy performance assessment of a window with a horizontal Venetian blind. Energy Build. 37, 836–843. https://doi.org/10.1016/j.enbuild.2004.11.008.

Shurcliff, W.A., 1980. Thermal Shutters and Shades: over 100 Schemes for Reducing Heat-Loss through Windows, first ed. Brick House Pub. Co., United States https://books.google.no/books?id=MQ5CAQAAIAAJ.

Soares, N., Costa, J.J., Samagaio, A., Vicente, R., 2014. Numerical evaluation of a phase change material-shutter using solar energy for winter nighttime indoor heating. J. Build. Phys. 37, 367–394. https://doi.org/10.1177/1744259113496388.

Tan, Y., Peng, J., Curcija, C., Yin, R., Deng, L., Chen, Y., 2020. Study on the impact of window shades' physical characteristics and opening modes on air conditioning energy consumption in China. Energy Built Environ 3, 254–261. https://doi.org/10.1016/j.enbenv.2020.03.002.

van Moeseke, G., Bruyère, I., De Herde, A., 2007. Impact of control rules on the efficiency of shading devices and free cooling for office buildings. Build. Environ. 42, 784–793. https://doi.org/10.1016/j.buildenv.2005.09.015.

Weinlaeder, H., Koerner, W., Heidenfelder, M., 2011. Monitoring results of an interior sun protection system with integrated latent heat storage. Energy Build. 43, 2468–2475. https://doi.org/10.1016/j.enbuild.2011.06.007.

Wright, J.L., Collins, M.R., Ned, T., 2008. Thermal resistance of a window with an enclosed Venetian blind: a simplified model. Build. Eng. 114 PART 1, 471–482.

Ye, Y., Xu, P., Mao, J., Ji, Y., 2016. Experimental study on the effectiveness of internal shading devices. Energy Build. 111, 154–163. https://doi.org/10.1016/j.enbuild.2015.11.040.

Zeyninejad Movassag, S., Zamzamian, K., 2020. Numerical investigation on the thermal performance of double glazing air flow window with integrated blinds. Renew. Energy 148, 852–863. https://doi.org/10.1016/j.renene.2019.10.170.

Zhang, C., Cheng, K., Wang, J., Xu, X., 2016a. Numerical evaluation of heat recovery performance of a switchable exhaust air window. Energy Proc. 88, 738–741. https://doi.org/10.1016/j.egypro.2016.06.056.

Zhang, C., Wang, J., Xu, X., Zou, F., Yu, J., 2016b. Modeling and thermal performance evaluation of a switchable triple glazing exhaust air window. Appl. Therm. Eng. 92, 8–17. https://doi.org/10.1016/j.applthermaleng.2015.09.080.